Effects of Flue Wall Deformation on Aluminum Anode Baking Homogeneity and Temperature Distribution

Mouna Zaidani [1], Rashid Abu Al-Rub[2], Abdul Raouf Tajik[3], Tariq Shamim[4]
1. Postdoctoral Researcher
2. Department Head and Associate Professor
3. Ph.D. Student
4. Professor
Institute Center for Energy (iEnergy), Department of Mechanical and Materials Engineering,
Masdar Institute of Science and Technology, Abu Dhabi, U.A.E.
Corresponding author: rabualrub@masdar.ac.ae

Abstract

The quality of anodes used in aluminum industry depends strongly on the baking process. It is essential to achieve a uniform temperature inside the anode during the baking process. Flue wall may deform during the service life of the furnace that may affects the baking process of the anodes and consequently reduce the quality of the anode. During furnace operation, the thermal expansion of flue walls is restrained due to the presence of headwalls that may promotes the deflection of flue walls. This study aims at investigating this phenomenon by developing a 3D model able to take into account a large number of physical phenomena and parameters that play a role in the baking process and affect the flue wall deformation process. This 3D model takes into account the thermo-hydro-mechanical coupling due to coupled fluid flow and transient heat transfer, packing coke load and the thermal expansion, the model is used to analyze the influence of these parameters on the resistance and deflection of the flue walls. This model can be used as a useful tool to study the effect of flue wall deflection on the aging of carbon anode furnaces.

Keywords: Baking process; aging; deflection; flue wall; thermo-hydro-mechanical coupling.

1. Introduction

The anode baking is the most expensive step in anode production. Fuel and refractory maintenance represent approximately 15% of total anode manufacturing cost. The baking of the anode is completed in an anode ring furnace. Such furnaces are composed of a number of sections with the anodes placed between flue walls into the pit. The firing zone is moving and the anodes remain stationary. Figure 1 shows a typical view of an open top furnace and a three-dimensional view of one section of the ring furnace. The whole furnace is made of a few such sections, forming an oval-shaped ring. Each section is divided into several pits with anodes stacked in each pit. In an aluminum type furnace, anodes are stacked in three layers. The pits are separated by pit walls, in which the hot gases flow. Approximately 100 anodes are loaded in each section. The anodes are surrounded by packing coke, which gives physical support and acts as a heat transfer medium. In the preheating and heating section, hot gases in the wall flues for transmission of heat through the brickwork and packing of coke to the anodes. In the cooling section, ambient air is used for cooling the anodes in a similar way. At the front of the fire, a chain of ring furnace sections operating in different parts of the baking cycle and linked together as a series of batch processes with a common gas flow between them, a draught fan maintains the gas flow through the chain of sections. Inflowing ambient air enters the last section in the fire train and is preheated by cooling the anodes. The heated air supplies oxygen for the combustion of oil in the heating sections. In the preheating sections, cold anodes are heated by hot gas and combustion of hydrocarbon volatiles coming from the binder pitch. Thus, the heat comes from combustion of

liquid or gaseous fuel as well as from hydrocarbon volatiles coming from the binder pitch. Thus, the heat comes from combustion of liquid or gaseous fuel as well as from the hydrocarbon volatiles, mainly tar, methane and hydrogen. Some heat also comes from combustion of the packing coke covering the anodes.

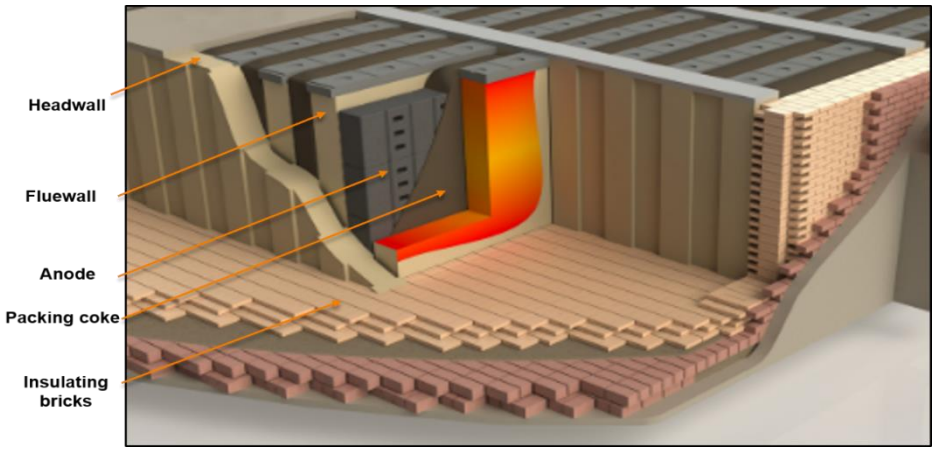

Figure 1. General overview of a typical anode baking furnace[1]

The quality of the anode used in the aluminum industry depends strongly on the baking process. In general, it is desirable to achieve a more uniform temperature inside the anode during the heating process. The aging of the baking furnace and the deformation of the flue and head walls lead among others to inhomogeneous baking of the anodes and consequently to a deterioration of the resulting anode quality[2, 3]. The development of a three-dimensional (3D) computational model able to take into account a large number of physical phenomena and parameters that play a role in the baking process and affect the flue wall aging process is needed.

Due to the huge dimension of the furnace and its very large time constant (in the order of months), it is not always possible to conduct physical experiments in order to determine the influence of the flue wall deformation on furnace's behavior and efficiency. The increasing interest in this topic has heightened the need for a mathematical model as a tool for predicting the influence of the flue wall aging on the anode baking homogeneity. However, few recent investigation studies have focused on the flue wall deformation modes, and how this deformation can affect the quality of the baked anodes [4, 5], the research has tended to focus on the process modeling considering a straight flue wall, and less attention has been paid to how the degree deformation of the baking furnace can affect the baking process efficiency.

In this study, we developed a 3D model that take into account the thermo-hydro-mechanical coupling due to coupled fluid flow, heat transfer and flue wall deformation. The fully coupled thermo-hydro-mechanical simulations were done by the finite element multi-physics commercial software COMSOL. Such 3D multi-physics modelling can be used as a powerful tool in the prediction of the effect of the flue wall deformation on the anode temperature distribution and homogeneity and thus predicting the anode baking quality. The present study gives useful insights for temperature distribution adjustment as a function of the flue wall and furnace design.

The life of carbon baking furnaces is usually limited by the deflection of its flue walls. This deflection as showed in Figure 2-a is promoted principally by the action of the headwalls which restrain the free thermal expansion of the flue walls, and by the action of the packing coke whose weight is partially supported by the flue walls. The resistance to deflection of the flue walls is a function of their rigidity [6]. In an open carbon baking furnace, the flue walls consist of firebricks linked together by mortar in horizontal joints. During service, the thermal expansion of flue walls consist of firebricks which are usually linked together by mortar. During service, the thermal

expansion of flue walls is restrained due to the presence of headwalls. This, as well as the effect of the load of the packing coke, promotes the deflection of the flue walls thus limiting their life [7].

The complex corrosion behavior of fireclay bricks is also a determined factor in the flue wall deterioration, the corrosion is determined by various individual interacting processes such as: migration of gases and melt, reduction of oxide brick components from the anode side and recrystallization processes. Sulphur, Sodium and fluorine containing compounds in particular react with the brick material. A melt is formed on the surface, which infiltrates the brick. Contaminated raw materials of the anodes and high temperatures on the anodes side enhance the formation of such a melt [8, 9]. In another hand, Due to the packing coke layer high ash content, it forms an iron–rich alumino-silicate slag on the flue wall (Figure 2-b). The slag layer acts as an additional protection again-burn of the uppermost anodes as well as of the coke. After the baking process, the slag must be removed separately [10]. The slag reacts with the refractory brick material, sticking firmly to it. With increasing fire cycles, more and more slag is enriched. Ultimately, sticking of coke particles to the slag-covered refractory brick walls leads to cracking. As a consequence of mechanical cleaning to remove the coke layer, slagger brick walls get quickly destroyed and must be repaired frequently. The repair of worn flues is a big cost factor in the maintenance of an open anode baking furnace. Essentially the influence of the deflection on the lifetime of the flues walls will be the focus of this work.

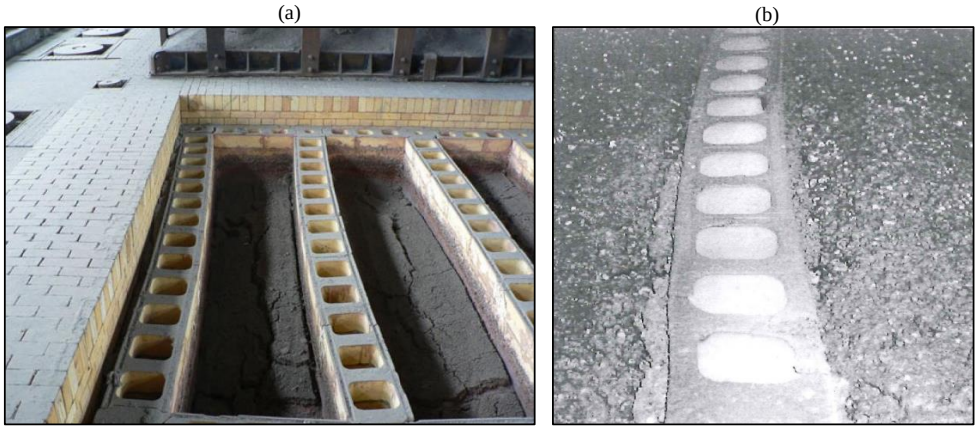

Figure 2. General view of (a) the flue wall deflection [11] and (b) Heavily slagged flue wall covered with metallurgical coke [10].

2. Model and computational method

2.1. Geometry model

A three-dimensional model was built comprising a typical section between the centerline of a flue and the centerline of a pit. Figure 3 present a schematic presentation of the geometry considered in the present study. In the flue, all baffles are represented in detail, tie bricks are not considered in this study. In the pit were placed 14 anodes of 1600 x 600 x 800 mm size, there are 2 domains, a solid domain composed of flue wall, packing coke and anodes, and a fluid domain for the gas flue. The thickness of the solids domain material layers, flue wall, packing coke and anodes in the direction of the pit length is 100 mm, 100 mm and 300 mm respectively. Symmetry was assumed on the centerline of the flue and the pit. This model is applied to one heating section in order to explore the effect of the flue wall deformation on the anode baking quality and temperature distribution homogeneity. In order to reduce the computational burden of simulating anode baking furnaces, several authors have used simplified models to account for the thermal energy released by combustion. In this study, the combustion process is simulated using a simplified hot air jet model, one of the simplest approaches is to eliminate the combustion model

in the simulations, and simply replacing the burner by an inlet of hot air [12], then, the effect of working condition on wall temperature distribution is deduced, In order to inject an amount of energy at the burners inlets equivalent to that injected with natural gas, the following strategy is used: The air is injected at the same temperature as the maximum flame temperature.

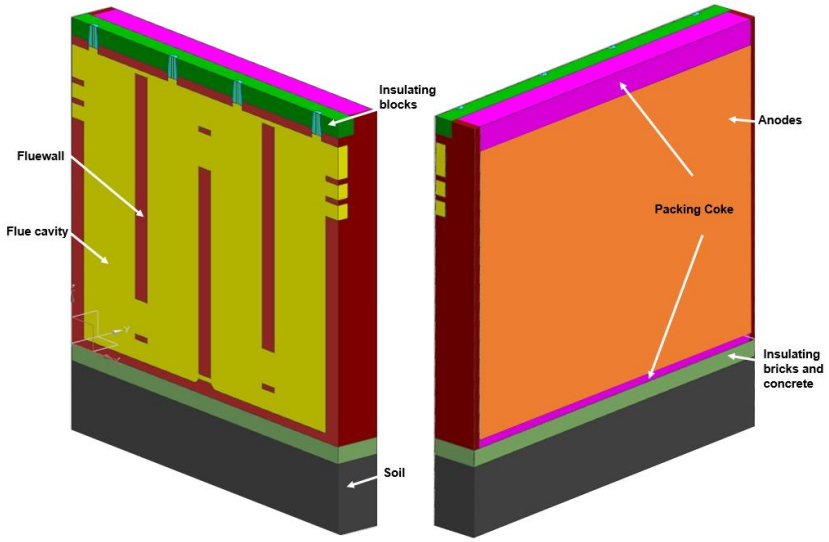

Figure 3. Schematic representation of the domains that is considered in the present study

The purpose of this work is to explore the application of a new thermo-hydro-mechanical model in the practical problems of anodes baking process using a deformable flue wall geometry and considering a different modes of flue wall deformation. This study will enable us to understand the influence of the flue wall deformation patterns on the anode baking homogeneity and to show how this model can be used for flue design and for optimization of the furnace lifetime.

The numerical model developed unable us to understand the effect of the flue wall deformation on the anode baking quality and temperature distribution homogeneity. The flue wall deflection modes used in this study (C shape) presented in figure (Figure 4) are qualitatively consistent with the flue wall deformation patterns (Figure 2). The present study gives useful insights for temperature distribution adjustment as a function of the flue wall and furnace design.

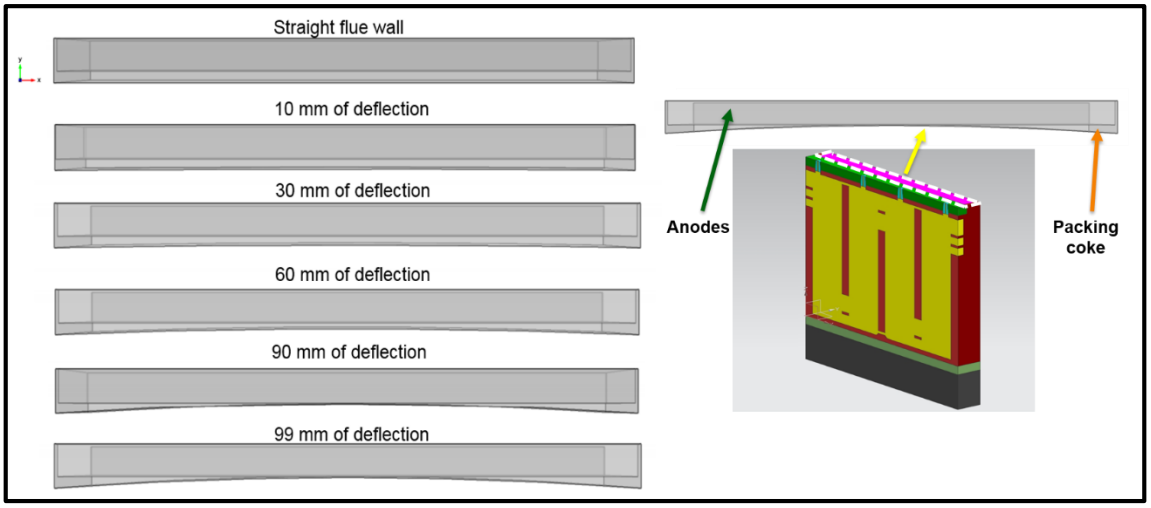

Figure 4. Schematic representation of the flue wall deflection modes that is considered in the present study.

2.2. Multiphysics mathematical model

As shown in Figure 5Figure 5, the deformation in the flue wall has a two-way link with temperature and the flue gas flow. Change in temperature during baking, for instance for the firing stage, would result in the development of thermal stresses in the brick wall, the generated stresses can cause undesired deformations or cracking in the flue wall and consequently altering its microscopic structure, and its thermal properties. This will not only progressively change the strength of the flue wall, but also will cause changes in the flow regime and the anodes baking quality.

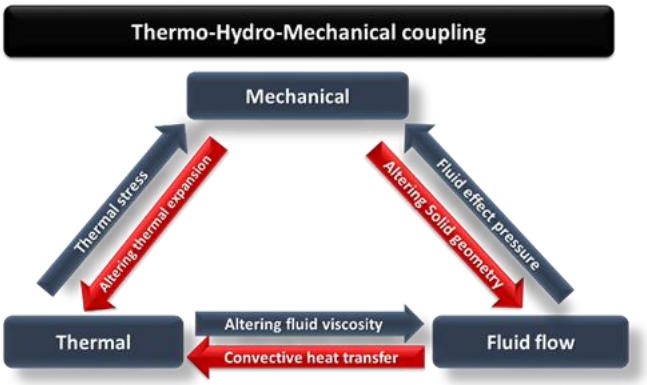

Figure 5. Flowchart of thermo-hydro-mechanical coupling of the flue wall.

In this work, we present a numerical framework that couples fluid, heat transfer. The numerical model was developed using the CDF commercial code COMSOL. Figure 6 shows an overview of the model of the baking furnace with an entire pit (solid domain) and the adjacent flues (gas flue domains). Phenomena that occur in the two parts of the furnace (solids and gas) are different so specific equations are solved in each part of the model through a virtual numerical interface. Thus, the global model of a baking furnace is divided into two sub-models: gas and pit (brick wall, packing coke, and anodes).

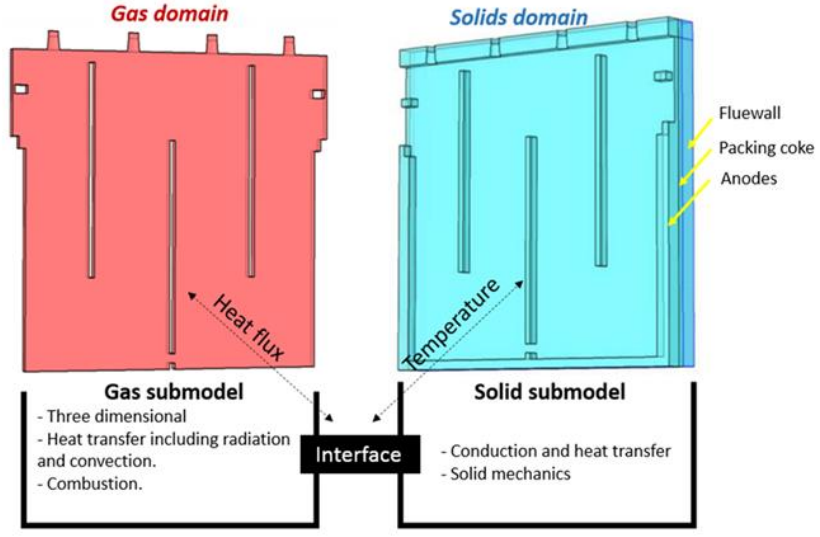

Figure 6. A schematic view of the flue and pit sub-models and their coupling.

These sub models are developed separately and then coupled through an interface at the flue wall surface on the flue side. This modular approach makes it easier to develop and modify each part. Also, if needed, each sub-model could be used exclusively for testing options in one part of the furnace (such as the flow distribution in the flue for a given geometry).On the gas part (flue), the

flow, heat transfer and mass transfer equations are solved. On the solid part, the heat transfer by conduction is solved, considering the thermal conductivity of various solids (flue wall, packing coke and the anodes). The model is steady state and calculates for one heating section.

In an anode baking horizontal flue ring furnace, the temperature distribution is one of the key factors influencing the quality of baked anodes and is closely correlated with the gas flow [13]. To understand the gas flow distribution in the flue, Navier-Stokes equations with turbulence model is adopted. The descriptions of incompressible gas flow are given as follow [14]:

$$\rho_g \nabla.\left(\boldsymbol{u}_g\right) = 0 \qquad (3)$$

$$\rho_g \frac{\partial u_g}{\partial t} + \rho_g (\boldsymbol{u_g}.\nabla)\boldsymbol{u_g} = \nabla.[-p\bar{\boldsymbol{I}} + (\mu + \mu_T)(\nabla \boldsymbol{u_g} + (\nabla \boldsymbol{u_g})^T)] \qquad (4)$$

$$\rho_g \frac{\partial \boldsymbol{k}}{\partial t} + \rho_g \left(\boldsymbol{u_g}\ .\nabla\right)\boldsymbol{k} = \nabla.\left[\left(\mu + \frac{\mu_T}{\sigma_k}\right)\nabla \boldsymbol{k}\right] + p_k - \rho_g \epsilon \qquad (5)$$

$$\rho_g \frac{\partial \epsilon}{\partial t} + \rho_g \left(\boldsymbol{u_g}\ .\nabla\right)\boldsymbol{\epsilon} = \nabla.\left[\left(\mu + \frac{\mu_T}{\sigma_\epsilon}\right)\nabla \boldsymbol{\epsilon}\right] + C_{\epsilon 1}\frac{\epsilon}{k}\, p_k - C_{\epsilon 2}\frac{\epsilon^2}{k}\epsilon\rho_g \qquad (6)$$

where $\mu_T = C_\mu \rho_g \dfrac{k^2}{\epsilon}$, $p_k = \mu_T\left[\nabla \boldsymbol{u} : \left(\nabla \boldsymbol{u} + (\nabla \boldsymbol{u})^{\boldsymbol{T}}\right)\right]$,

u_g refers to the gas velocity; k is the turbulent kinetic energy; ϵ the turbulent dissipation rate; p pressure; ρ_g denotes gas density; μ molecular viscosity; μ_T effective viscosity; σ_k and σ_ϵ are Prandlt number; p_k, $C_{\epsilon 1}$ and $C_{\epsilon 2}$ are constants [15].

Heat from the gas in the flue is transferred to the brick wall surface by convection and radiation, then by conduction from the flue wall surface into the bricks, and on to the packing coke, then the anodes. By combining Fourier's law and energy conservation law, the heat transfer through the solid can be represented in the following form, called transient heat conduction equation:

$$\rho_s C_p \frac{\partial \boldsymbol{T_s}}{\partial t} = \lambda_s \nabla \boldsymbol{T_s} - Q_s \qquad (7)$$

T_s is the solids (anodes, packing coke and flue wall) temperature, and λ_s is the thermal conductivity. Q_s represents the thermal loss to the atmosphere by coke and the foundation, heat is exchanged by Radiation and convection following the relationship:

$$-n.\left(-\lambda \nabla \boldsymbol{T}\right) = \omega\sigma\left(T_\infty^4 - T^4\right) + h_{equiv}\left(T_\infty - T\right) \qquad (8)$$

At the brick wall surface, where solids and flue gases are in contact, heat is exchanged following the relationship:

$$q' = \left(h_C + h_R\right)\left(T_g - T_W\right) \qquad (9)$$

where q' is the heat flux through the fluid-solid interface; h_c is the convection heat transfer coefficient between the flue wall and the gas; h_R is the radiation heat transfer coefficient between the flue wall and the gas flue; T_W is the flue wall temperature at the boundary; T_g is the gas temperature.

The convection heat transfer coefficient is determined by the Dittus-Boelter correlation [16]:

$$h_C = \left(\frac{\lambda_g}{D_h}\right)0.023\, Re^{0.8} Pr^{\gamma} \qquad (10)$$

where λ_g is the thermal conductivity of gas; D_h is the representative hydraulic diameter inside the flue, Pr is Prandlt number of gas; γ is an exponent, Re is the Reynolds number of the flow. The

radiation heat transfer coefficient is given by [6]:

$$h_R = \sigma\left(\frac{w_g T_g^4 - \eta_g T_w^4}{T_g - T_W}\right) \qquad (11)$$

where σ is the Stephan-Boltzmann constant= $5{,}67 \times 10^{-8}$ $[W.m^{-2}.K^{-4}]$; ω_g and η_g are the emissivity and the absorptivity of mixed gas, respectively.
As showed in Figure 7-a, at symmetry, the boundary conditions applied are:

- ✓ Heat transfer symmetric boundary conditions:

At symmetries, heat flux equals zero.

$$-n.\left(-\lambda_S \,.\nabla \boldsymbol{T_S}\right) = 0 \qquad (12)$$

- ✓ Fluid flow symmetric boundary conditions:

At symmetry, there is no flow normal to the symmetric boundary, mathematically this is means that we specify that,

$$\boldsymbol{u_g}.n = 0 \qquad (13)$$

$$\nabla \boldsymbol{K}.n = 0, \quad \nabla \epsilon.n = 0 \qquad (14)$$

Where n is the normal vector pointing to the boundary outside, T_s is the solid temperature, u_g is the gas velocity.Viscosity are assumed to remain constant at values corresponding to air at the inlet at 800°C.Thermal conductivity and viscosity are assumed constant and as a function of temperature, in this study both cases are explored. As showed in Figure 7-b, mesh is constituted of about 83123 tetrahedral elements and 22662 Triangular elements. Consequently, the complete 3D mesh typically contains 100000 elements. A hot jet air approaches is considered to include the energy generated by the natural gas combustion in order to reduce the computational burden of simulating anode baking furnaces and simply replacing the burner by an inlet of hot air at -20 Pa. In order to inject an amount of energy at the burners inlets equivalent to that injected with natural gas, the following strategy is used: The air is injected at the same temperature as the maximum flame temperature (1800°C). Although this strategy does not provide any information in order to improve combustion efficiency and reduce natural gas consumption, but it is interesting to document the ability of this simple approach to provide realistic anode temperature evolution and predict anode variability with the help of the hot air jet model.

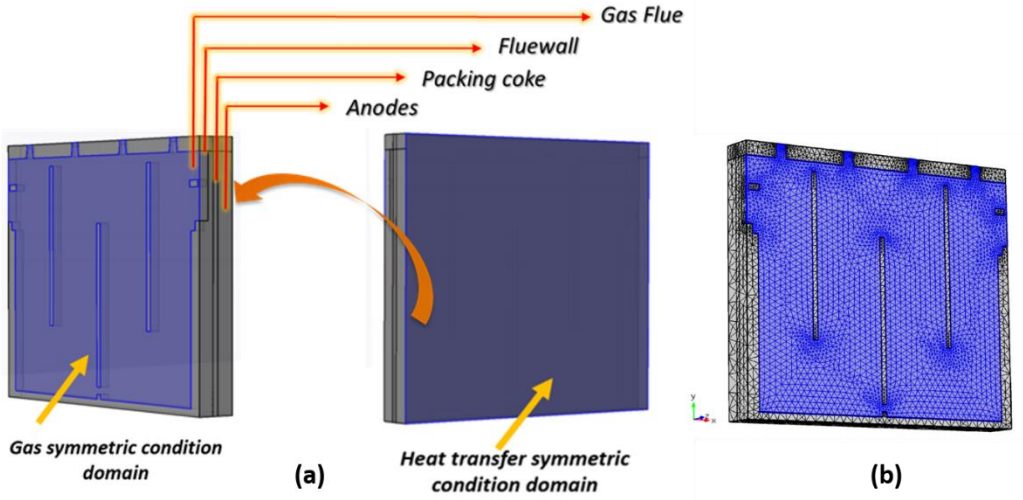

Figure 7. A schematic representation of (a) the model domain if symmetry could be assumed, (b) the domains meshing that is considered in the present study.

In this study, two cases are presented. In case 1, the solid thermal conductivity and specific heat (anodes and packing coke) are assumed varying as a function of the temperature, based on

experimental data. Using a linear extrapolation, we can extract the values of anodes and packing coke thermal conductivity corresponding to a temperature value bellow 20°C and above 1000°C for the packing coke and 1200°C for the anodes. In case 2, thermal conductivity and viscosity for the anodes and the packing coke are assumed to remain constant by considering the average value for the temperature above 500°C corresponding to the temperature in the firing section. In this study both cases are explored. The Table 1summarizes the materials properties used in this study.

Table 1. Material properties used in this study.[16]

Materials properties as a function of temperature

Materials	Temperature (C)	Thermal conductivity ($W.m^{-1}.K^{-1}$)	Specific heat ($J.Kg^{-1}.K^{-1}$)	Density (Kg/m^3)
Flue wall		1.46	965	2490
Packing coke	20	0.87	652	1240
	100	0.87	941	
	300	0.95	1374	
	500	1.08	1650	
	700	1.24	1816	
	1000	1.50	2000	
Anodes	20	2.55	871	1545
	200	2.45	1105	
	500	3.75	1291	
	700	4.55	1311	
	850	5.30	1414	
	1000	6.05	1519	
	1200	7.00	1700	

Constant material properties

Materials	Thermal conductivity ($W.m^{-1}.K^{-1}$)	Specific heat ($J.Kg^{-1}.K^{-1}$)	Density (Kg/m^3)
Flue wall	1.46	965	2490
Packing coke	1.27	1822	1240
Anodes	5.33	1447	1545

3. Results and discussions

The main purpose of this work is to explore the application of a new thermo-hydro-mechanical model in the practical problems of anodes baking process using a deformable flue wall geometry and considering different modes of flue wall deformation from a 0 mm of deflection for a straight flue wall to a 99 mm deflected flue wall. This model is applied to one heating section in order to explore the effect of the flue wall deformation on the temperature distribution homogeneity within this section. Process modelling is not the focus of this work. Flue wall design modelling and its deformation and its effect on the creation of hot spots and anode overbaking in certain areas is the main purpose of this study, the reason for which the other sections are not considered in this current work. This study will enable us to understand the influence of the flue wall deformation patterns on the anode baking homogeneity and to show how this model can be used for flue design and for optimization of the furnace lifetime.

Figure 8 presents the temperature distribution temperature at the packing coke interface (Figure 8-a) and for the anode middle plane (Figure 8-b) as a function of the flue wall deflection and for temperature dependent material properties. The anode temperature mapping is displayed for the different deformation modes, from a 0 mm deflection for a straight flue wall to a 99 mm deflected flue wall. As can be clearly seen in figure 4.14, the anode temperature patterns obtained in this study is qualitatively similar to the anode temperature distribution presented in the literature [12]. The warmest zone is located near to the outlet and the second burner position for all cases study, and the coldest zone near to the inlet. Moving from a straight flue wall to a deflected flue wall, we can clearly see that the warmest zone are getting warmer in the packing coke-anode interface (Figure 8-a) and a creation of a hot spots at the anode middle-plane interface (Figure 8-b). The anode temperature is increasing by the increase of the flue wall deformation. For the packing coke-anode interface (Figure 8-a), the interface average temperature is around 892°C for a straight

flue wall and increase to reach 900°C for a 99 mm deflected flue wall. Moving from the packing coke-anode interface to the anode middle-plane (Figure 8-b), the heat diffusion in the solids has smoothed further the hot For the anode middle plane, the middle plane average temperature is around 890°C for a straight flue wall, it increases to reach 897.7°C for a 99 mm deflected flue wall

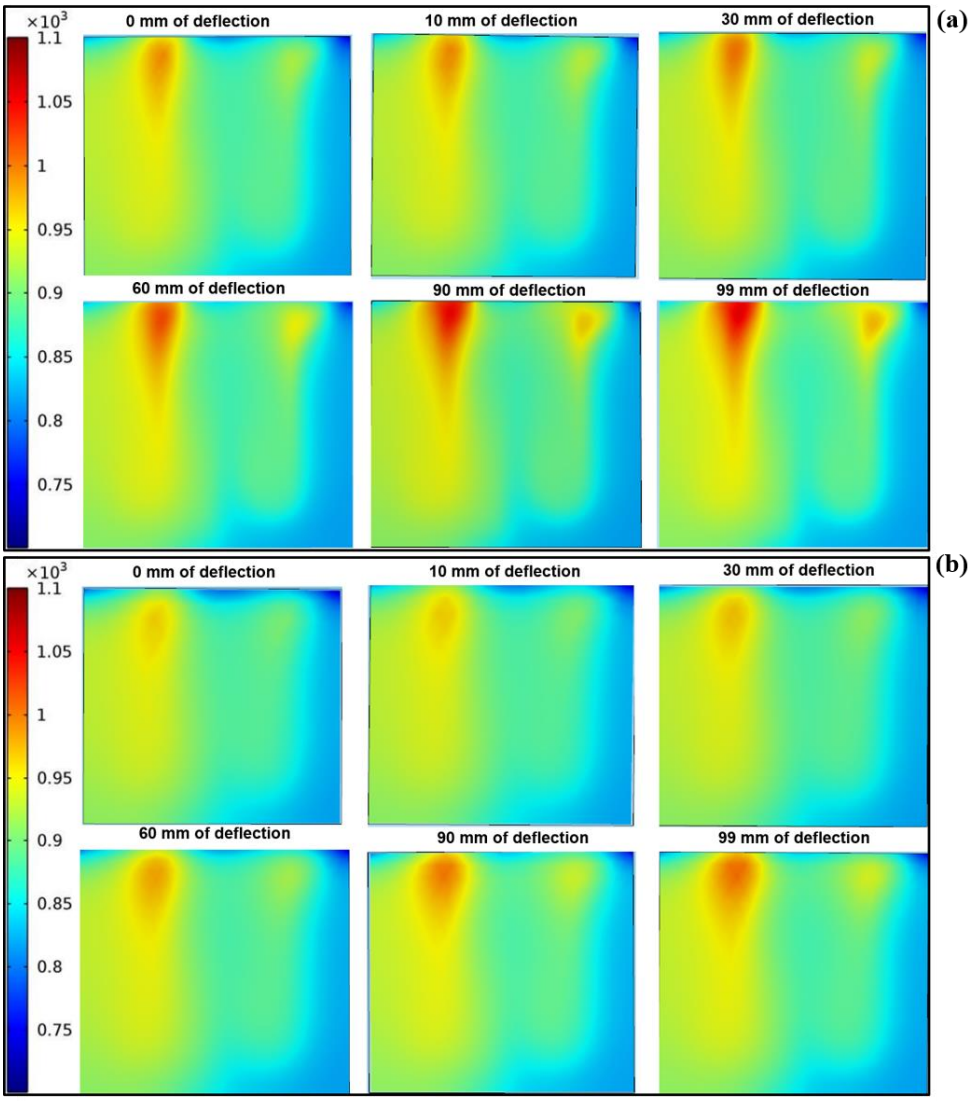

Figure 8. Anode map temperature at the packing coke interface (a) and the anode middle plane (b) as a function of the flue wall deflection.

The anode maximum temperature is increasing from 992°C to 1056°C for a straight flue wall and a 99 mm deflected flue wall respectively. The more the flue wall is deflected, the higher is the anode temperature leading to an overbaking of the anodes in a certain spots and consequently to an inhomogeneous anodes baking. The homogeneity of the temperature can be presented by the range of temperature (the difference between the maximum and the minimum temperature of the anode), the range presented in Table 2 clearly shows that the range is increasing from 275°C for a straight flue wall to 319°C for a 99 mm deflected flue wall. More details about the anode temperature distribution as a function of the flue wall deformation modes is displayed in Table 2.

Figure 9-a shows the evolution of the Anode average temperature, at the anode middle plane and at the packing coke- anode interface as a function of the flue wall deflection. (0, 30, 60, 90 and

99mm). It can be observed that the anode volume average temperature is increasing by the increase of the flue wall deflection from 891°C to 898.5°C for a straight and a 99 mm deflected flue wall, respectively. As expected, the anode middle-plane average temperature is lower than the average temperature at the middle plane. At the anode packing coke-interface, the anode average temperature increase from 892°C for a straight flue wall and reach 900°C for a deflected flue wall. The anode middle-plane temperature is increasing from 890°C to 897.7°C for a straight flue wall and 99mm deflected flue wall, respectively.

Table 2. The anode temperature at the packing coke interface and the middle plane as a function of the flue wall deflection.

Anode temperature distribution	Case 1 (0 mm)	Case 2 (10 mm)	Case 3 (30 mm)	Case 4 (60 mm)	Case 5 (90 mm)	Case 6 (99 mm)
Maximum temperature (°C)	992.3	996.3	1003.6	1021.1	1052.5	1056.6
Minimum temperature (°C)	716.8	720.5	721.9	728.21	735.4	737.9
Maximum-Minimum (°C)	275.5	275.8	281.7	292.89	317.1	318.7
Volume Average temperature (°C)	891.1	891.6	892.3	893.7	896.53	898.5
Average temperature (°C) Flue cavity side	892.3	892.6	893.7	895.15	897.9	899.9
Average temperature (°C) Mid plane	889.9	890.1	891.4	892.8	895.03	897.7

Figure 9-b depicts the anode volume average, minimal and maximal temperature as a function of the flue wall deflection, the anode maximum temperature is increasing from 992°C to 1056°C for a straight flue wall and a 99 mm deflected flue wall, respectively. The anode minimum temperature is increasing from 716.8°C to 738°C for a straight flue wall and a 99 mm deflected flue wall, respectively. The homogeneity of the temperature can be presented by the range of temperature (the difference between the maximum and the minimum temperature of the anode), the range is increasing from 275°C for a straight flue wall to 318.7°C for a 99 mm deflected flue wall leading to an inhomogeneous anodes baking.

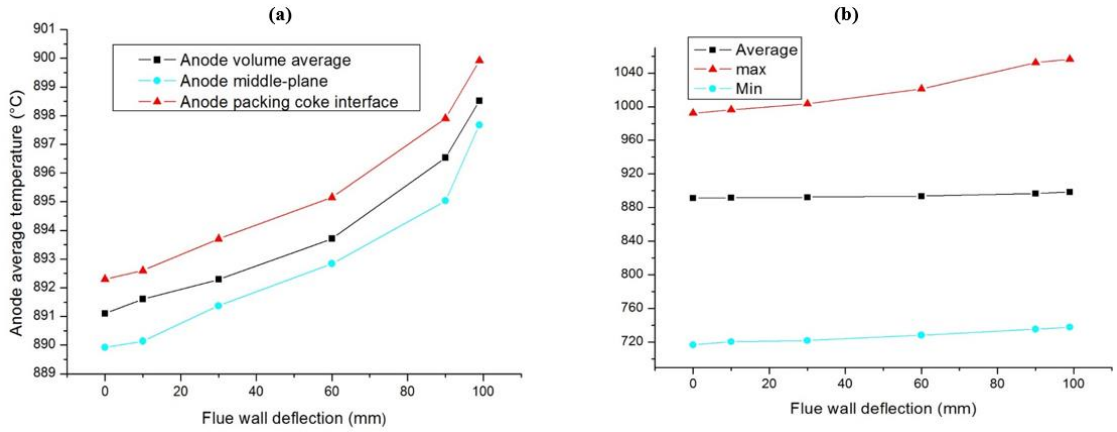

Figure 9. The temperature variation as a function of deflection of (a) the Anode volume average, the anode middle plane and at the packing coke interface (b) The anode volume average, minimal and maximal temperature.

In some case study, it is difficult to obtain the evolution of the materials properties as a function of temperature. In order to evaluate the effect of materials properties on the anode temperature distribution as a function of the flue wall deflection, we presents the anode temperature distribution for a constant materials properties. Figure 10 presents the temperature distribution Temperature at the packing coke interface (Figure 10-a) and for the anode middle plane (Figure

10-b) as a function of the flue wall deflection. The anode temperature mapping is displayed for the different deformation modes, from a 0 mm deflection for a straight flue wall to a 99 mm deflected flue wall.

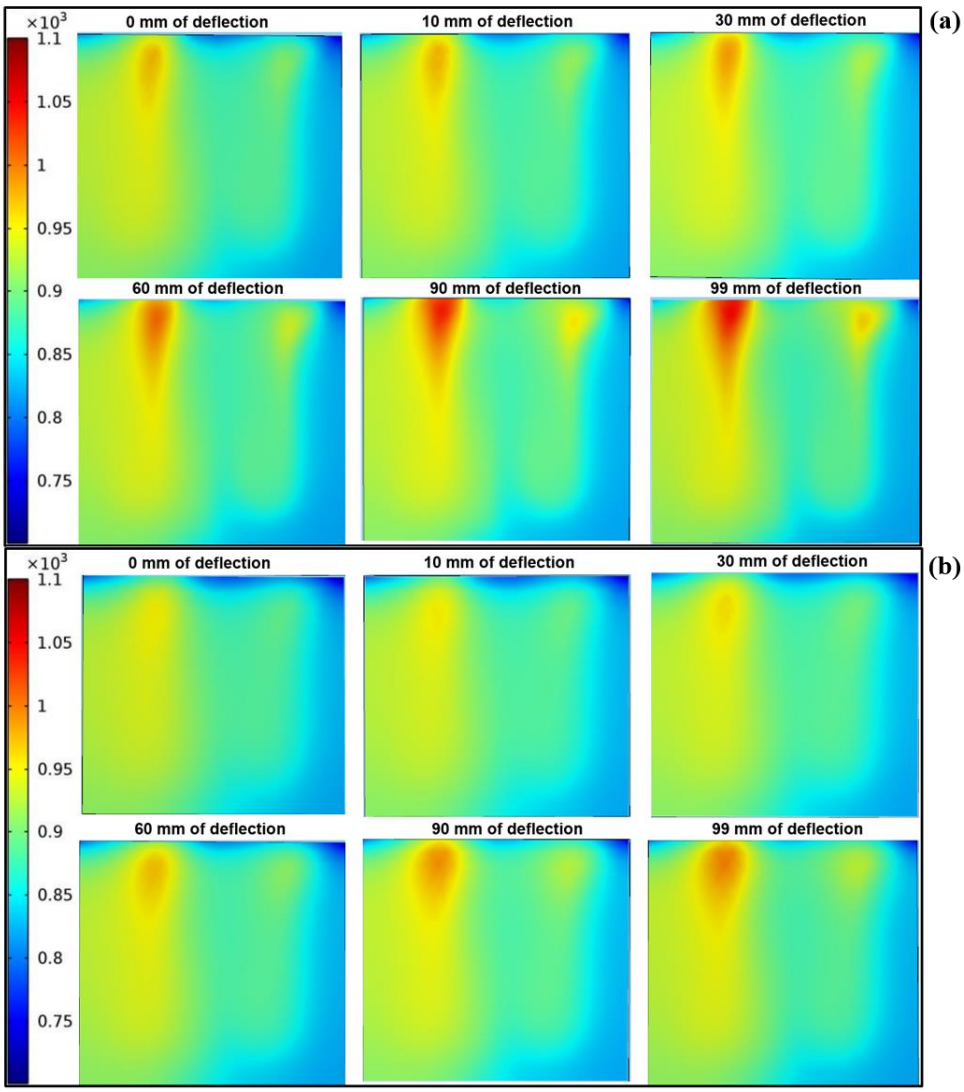

Figure 10. Anode map temperature at the packing coke interface (a) and the anode middle plane (b) as a function of the flue wall deflection (Constant material properties).

Table 3. The anode temperature at the packing coke interface and the middle plane as a function of the flue wall deflection (constant material properties).

Anode temperature distribution	Case 1 (0 mm)	Case 2 (10 mm)	Case 3 (30 mm)	Case 4 (60 mm)	Case 5 (90 mm)	Case 6 (99 mm)
Maximum temperature (°C)	975.9	978.3	988.4	1007.04	1032.2	1047.3
Minimum temperature (°C)	714.2	716.1	719.3	725.8	731.2	735.9
Maximum-Minimum (°C)	261.7	262.2	269.1	281.4	301	311.4
Volume Average temperature (°C)	887.3	887.9	889.09	891	894.9	896.5
Average temperature (°C) Flue cavity side	888.8	889.3	890.6	892.5	896.9	898
Average temperature (°C) Mid plane	886.3	886.7	888.1	890.05	894.4	895.5

As can be clearly seen in Figure 10, the warmest zone is located near to the outlet and the second burner position for all cases study, and the coldest zone near to the inlet. Moving from a straight flue wall to a deflected flue wall, we can clearly see that the warmest zone is getting warmer in the packing coke-anode interface (Figure 10-a) and a creation of a hot spots at the anode middle-plane interface (Figure 10-b). The anode temperature is increasing by the increase of the flue wall deformation. For the packing coke-anode interface (Figure 10-a), the interface average temperature is around 888°C for a straight flue wall and increase to reach 898°C for a 99 mm deflected flue wall. Moving from the packing coke-anode interface to the anode middle-plane (Figure 10-b), the heat diffusion in the solids has smoothed further the hot for the anode middle plane, the middle plane average temperature is around 886°C for a straight flue wall, it increases to reach 895°C for a 99 mm deflected flue wall. More details about the anode temperature distribution as a function of the flue wall deformation modes is displayed in Table 3.

Figure 11 displays a comparison between the anode volume average temperature as a function of the flue wall deflection for dependent and independent material properties. It can be observed that there is a deviation in the results of the anodes average temperature between the two case study. The range of deviation is larger for the lowest temperature value, and the range get smaller as the temperature getting higher. This pattern could be due to the fact that in the present study the constant material properties assumed to remain constant by considering the average value for the temperature above 500°C giving a more accurate results for the higher temperature value. However, using a constant material properties leads to a misleading conclusions regarding the anode temperature distribution and the creation of hot spot in the anodes.

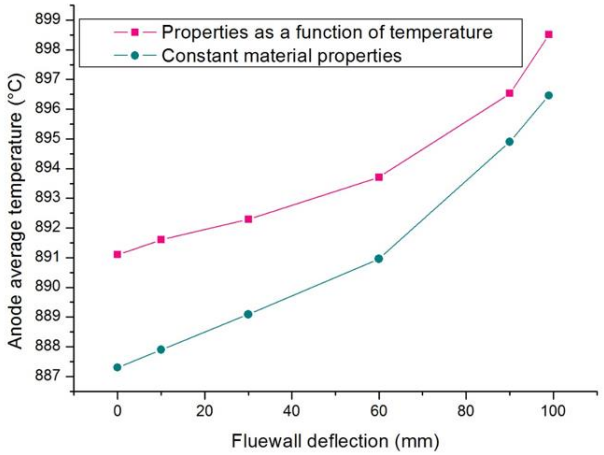

Figure 11. The anode volume average temperature as a function of the flue wall deflection for constant and variables material properties.

4. Conclusions

Flue-wall's aging is usually accompanied by its deformation. Such deformations creates difficulties in loading and unloading anodes in the pits and to inhomogeneous anode baking. In this work, we developed a tool that can predict the anode temperature distribution, creation of hot spot and anode overbaking in certain area as a function of the flue wall deformation mode. It has been showed that using the correct material properties is essential for a realistic prediction of the anode temperature distribution. By developing this tool, we can effectively predict the deformable flue wall reliability under varying operating conditions, and provide useful insights on enhancing the long-term structural integrity through furnace retrofitting or design adjustment. In the future, other flue wall deformation modes will be studied, the main purpose is to explore all the realistic flue wall deformation patterns, and how it affects the anode baking homogeneity, in order to establish a flue wall deformation modes database linked to the consequence on the anode baking quality

Acknowledgements

We acknowledge the support from the Emirates Global Aluminium (EGA).

5. References

1. F.G. Friedherz Becker, Ring Pit Furnaces for Baking of high quality anodes. *An Overview. Riedhammer, in.*
2. D.S. Severo, V. Gusberti and E.C. Pinto, Advanced 3D modelling for anode baking furnaces, The minerals, *Metals and Materials society*, (2005), 697-702.
3. P F. Goede, Refurbishment and modernization of existing anode baking furnaces, *Light metals, The minerals, Metals and Materials society*, (2007), 973-976.
4. M. Baiteche et al., Description and application of the 3D mathematical model for horizontal anode baking furnaces, *Light Metals 2015*, 1115-1120.
5. Y. Kocaefe et al., Different mathematical modelling approaches to predict the horizontal anode baking furnace performance, *11th AustralAsian Aluminium Smelting Technology Conference*, 2014, 15 pages.
6. Frank P. Incropera, David P. DeWitt, Fundamentals of Heat and Mass Transfer, *4th Edition, Chapter 9*, in, 1996.
7. C. Allaire, Effect of the type of brick and mortar on the resistance to deflection of the flue walls in horizontal flue carbon furnaces, *Light Metals* 1994, 551-564.
8. P. Quirmbach, *Private communication with author*, RWTH Aachen, 30 August, 1994.
9. Brunk Fred, Corrosion and behaviour of fireclay bricks used in the flues of open anode baking furnaces. *Light Metals 1995*, 641-646.
10. H.L. Fred Brunk, Improved anode baking furnace cover material, *Light Metals* 2002, 629-632.
11. A. Yurkov, Refractories for aluminium, DOI 10.1007/978-3-319-11442-2-4. *Springer International Publishing Switzerland*, 2015.
12. Francois Gregoire, Louis Gosselin, Combustion in anode baking furnaces : Comparison of two modeling approaches to predict variability, *Proceedings of combustion institute-Candian section, Spring Technical Meeting*, Universite Laval. May 13-16, 2013.
13. P. Zhou et al., Simulation of the influence of the baffle on flowing field in the anode baking ring furnace, *Journal of Central South University of Technology*, 9 (2002) 208-211.
14. T. Wen-quan et al., Numerical heat transfer, *Xi'an Jiaotong University Press*, (1988).
15. Jian-ren et al., The theory and computation on gas and solid multi-phase flow in engineering [M] *Hangzhou: Zhejiang University Press*, (1990).
16. D.S. Severo, V. Gusberti, User-friendly software for simulation of anode baking furnaces. , in: *Proceeding of 10th Australisian*, 2011.